Article

Discovery Medicine 2025; 37(203): 2932–2941
https://doi.org/10.24976/Discov.Med.202537203.245

Role of USP16 in Aβ1–42-Induced Alzheimer's Disease: Targeting IFI16 to Alleviate the Inflammatory Response

Bo Cui[1], Yan Ding[1], Cunjiang Li[1,*]

[1]Department of Neurology, Xuanwu Hospital Capital Medical University, 100053 Beijing, China
*Correspondence: licunjianglcj222@163.com (Cunjiang Li)
Submitted: 15 August 2025 Revised: 26 September 2025 Accepted: 31 October 2025 Published: 20 December 2025

Background: Alzheimer's disease (AD) is a progressive neurodegenerative disorder characterized by β-amyloid (Aβ) accumulation, neuroinflammation, and neuronal loss. Interferon gamma-inducible protein 16 (IFI16) regulates inflammatory processes in AD, while ubiquitin-specific peptidase 16 (USP16) has been shown to ameliorate memory deficits in AD models. This study aimed to elucidate the interplay between USP16 and IFI16 in AD pathogenesis.

Methods: Differentially expressed genes associated with AD were identified using dataset GSE129296. Glial cells were exposed to β-amyloid peptide (Aβ)1–42 to establish an *in vitro* AD model, followed by indirect co-culture with neuronal cells. Neuronal viability and apoptosis were evaluated using the Cell Counting Kit-8 assay and flow cytometry, respectively. Levels of tumor necrosis factor (TNF)-α and interleukin (IL)-1β in model glial cells were quantified by Enzyme-linked immunosorbent assay (ELISA). A potential deubiquitylating enzyme of IFI16 was predicted using Ubibrowser and confirmed by co-immunoprecipitation, while the ubiquitination levels of IFI16 were assessed. The expression of USP16/IFI16 and toll-like receptor 4 (TLR4)/NLR family pyrin domain containing 3 (NLRP3) was determined by reverse transcription-quantitative PCR (RT-PCR) and western blotting.

Results: IFI16 was markedly upregulated in AD. Silencing of IFI16 attenuated Aβ1–42-induced proinflammatory responses in glial cells, reduced neuronal apoptosis, and enhanced neuronal viability, accompanied by decreased inflammatory cytokine levels and downregulation of TLR4/NLRP3 expression. USP16, identified as the deubiquitylating enzyme of IFI16, was significantly elevated in Aβ1–42-stimulated glial cells, and its silencing reduced IFI16 expression. Furthermore, IFI16 overexpression reversed the effects of USP16 knockdown on cell survival, apoptosis, and inflammation.

Conclusion: USP16 depletion alleviates inflammation and apoptosis in AD cellular models through modulation of IFI16, suggesting that USP16 may serve as a promising therapeutic target for AD.

Keywords: Alzheimer's disease; ubiquitin specific peptidase 16; interferon gamma-inducible protein 16; inflammation; TLR4/NLRP3 axis

Introduction

Alzheimer's disease (AD) is a neurodegenerative disorder that impairs cognitive development and neurocognitive function, neuropathologically featured by neurodegeneration, neuronal loss, and the formation of neurofibrillary tangles and β-amyloid peptide (Aβ) plaques [1]. AD progresses along a continuum, beginning from an asymptomatic preclinical phase to mild cognitive impairment, and eventually to mild, moderate, and even severe dementia [2]. At present, only two classes of drugs have been approved for AD treatment; however, these agents merely alleviate AD-related symptoms rather than cure or prevent the disease [3]. Several essential elements of AD pathophysiology have been identified as critical contributors, driving the translation of these findings into potential therapeutic strategies [4].

Growing evidence has underscored the role of neuroinflammation in neurodegenerative diseases (NDs) such as AD [5]. For example, the pathogenesis of AD is not only confined to the neuronal compartment but also involves strong interactions with immunological mechanisms within the brain [6]. Notably, communication between neurons and glial cells is essential for maintaining synaptic homeostasis and may be disrupted during AD progression [7]. In light of this, we aimed to identify candidate molecules that may modulate neuroinflammation in AD. We first analyzed differentially expressed genes (DEGs) using the GSE129296 dataset (expression data from microglia in Aβ and Tau mouse models of AD). Among the top three cross-referenced genes, interferon gamma-inducible protein 204 (IFI204), the murine homolog of interferon gamma-inducible protein 16 (IFI16), was found to be markedly elevated in AD [8]. IFI16 (also known as p204) plays a pivotal role in canonical lipopolysaccharide (LPS)-induced toll-like receptor 4 (TLR4) signaling, which can bind to Aβ and activate downstream intracellular signaling cascades such as NLR family pyrin domain containing 3 (NLRP3), thereby amplifying inflammation in AD

[9–11]. Hence, it is reasonable to hypothesize that IFI16 may exacerbate neuroinflammation in AD by modulating the TLR4/NLRP3 signaling pathway.

We then investigated the specific mechanisms underlying this process. As a post-translational modification (PTM) essential for maintaining multiple physiological processes, protein ubiquitination allows cells to mount rapid and adaptive responses to various stimuli [12,13]. Meanwhile, disruption of the ubiquitin-proteasome system (UPS) in AD has been observed, wherein UPS dysfunction contributes to the accumulation of phosphorylated tau (p-tau), an underappreciated marker of AD [14]. Moreover, ubiquitin has been shown to modulate various aspects of protein fate and function, including protein degradation via the UPS [15]. Conversely, deubiquitylation, the reverse process, is catalyzed by deubiquitinating enzymes (DUBs) that remove ubiquitin from the ubiquitinated substrates, and DUBs have emerged as promising therapeutic targets in neurodegenerative diseases (NDs), including AD, due to their roles in modulating the stability of NDs-associated pathological proteins [16,17].

Based on these findings, we hypothesized the presence of potential candidates capable of mediating the deubiquitylation and stabilization of IFI16, thereby exacerbating neuroinflammation in AD. Thus, we predicted the upstream mediator with the potential to deubiquitinate IFI16. Among the predicted deubiquitylating enzymes, only ubiquitin-specific peptidase 16 (USP16) stood out, as inhibition of USP16 has been reported to rescue stem cell aging and ameliorate memory deficits in an AD model [18]. Therefore, this study aimed to determine whether USP16 also mediates the deubiquitylation of IFI16, thereby worsening neuroinflammation in AD.

Materials and Methods

Bioinformatics

The dataset GSE129296 (https://www.ncbi.nlm.nih.gov/geo/query/acc.cgi?acc=GSE129296) was retrieved from the Gene Expression Omnibus (GEO) database and analyzed using the GEO2R tool in the NCBI (https://www.ncbi.nlm.nih.gov/geo/geo2r/). The resulting differential expression data were visualized as a volcano plot.

Additionally, Ubibrowser (http://ubibrowser.bio-it.cn/ubibrowser_v3/) was adopted to predict potential deubiquitylation enzymes targeting IFI16, and the corresponding data were presented in the figures.

Cell Culture and Intervention

The human glial cell line HMC3 (CRL-3304) and the neuronal cell line SH-SY5Y (CRL-2266) were obtained from the American Type Culture Collection (ATCC, Manassas, VA, USA). Cells were maintained in ATCC-formulated Eagle's Minimum Essential Medium (EMEM, 30-2003, ATCC, USA) supplemented with 10% bovine calf serum (30-2020, ATCC, USA), with or without F12 medium (10-080-CV, Corning, Inc., Corning, NY, USA). The human embryonic kidney cell line HEK-293T (CRL-3216) was also obtained from ATCC and cultured in Dulbecco's Modified Eagle's Medium (DMEM, 30-2002, ATCC, USA) supplemented with 10% bovine calf serum and 2 mM L-glutamine (30-2214, ATCC, USA). All cell lines were maintained in an incubator (NU-5720, NuAire, Plymouth, MN, USA) at 37 °C with 5% CO_2. All lines were tested for mycoplasma contamination, confirmed to be free of contamination, and were authenticated using short tandem repeat (STR) analysis.

For transfection, sequences targeting USP16 and IFI16 were inserted into short hairpin RNA (shRNA) expression vectors pGPU6 (C02001, GenePharma, Shanghai, China), while random sequences were cloned into the corresponding negative control vector (C03002, GenePharma, Shanghai, China). All sequences used are listed in Table 1. Meanwhile, the full-length IFI16 coding sequence was ligated into the pcDNA 3.1 expression vector (V790-20, Invitrogen, Carlsbad, CA, USA), with the empty vector serving as the negative control.

Table 1. Sequences used for transfection.

Gene	Sequence (5′-3′)
sh*IFI16* #1	GCTACTTCACCTGCACCCT
sh*IFI16* #2	GGAGAAATTCAATGGAAAG
sh*IFI16* #3	GGAAGGGAGTCATTTTCCA
sh*USP16* #1	GGAATCAAAAGGGCAGTGG
sh*USP16* #2	GCTATCAGCAGCAAGACAG
sh*USP16* #3	GACAATAAAGTGAAAGATA
sh-NC	CAACAAGATGAAGAGCACCAA

shIFI16, short hairpin RNA targeting interferon gamma-inducible protein 16; shUSP16, short hairpin RNA targeting ubiquitin-specific peptidase 16; sh-NC, negative control of short hairpin RNA.

The constructed shRNA expression vectors and IFI16 overexpression plasmids were transfected into HMC3 glial cells with or without Aβ1–42 exposure using Lipofectamine 2000 transfection reagent (11668-027, Invitrogen, Carlsbad, CA, USA) at 37 °C for 48 h according to the manufacturer's instructions. Following transfection, the cells were harvested for subsequent analyses.

For the intervention with Aβ1–42 to mimic the AD model, all procedures for preparing oligomeric Aβ1–42 solution followed a previously described protocol [19]. Briefly, 1 mM Aβ1–42 (A99268, Acmec Biochemical, Shanghai, China) was first dissolved in 100% hexafluoroisopropanol (HFIP, H30760, Acmec Biochemical, China). HFIP was then evaporated using a SpeedVac™ SRF110 refrigerated centrifugal vacuum concentrator (SRF110P1-115, ThermoFisher Scientific, Waltham, MA, USA). The resulting, peptide film was resuspended

to a concentration of 5 µM in anhydrous dimethyl sulfoxide (DMSO, D12345, ThermoFisher Scientific, USA), and subsequently diluted with phosphate-buffered saline (PBS, AC13317, Acmec Biochemical, China) to a final concentration of 400 µM, followed by the addition of 0.2% sodium dodecyl sulfate (SDS, S19770, Acmec Biochemical, China). The prepared solution was incubated at 37 °C for 24 h, then further diluted with PBS to 100 µM and incubated for an additional 24 h. Based on previous studies [19], treatment with 5 µM Aβ1–42 for 24 h was performed for subsequent experiments.

Enzyme-Linked Immunosorbent Assay (ELISA)

The levels of proinflammatory cytokines tumor necrosis factor (TNF)-α and interleukin (IL)-1β were quantified using their corresponding ELISA assay kits (RK00030, RK00001, ABclonal, Wuhan, China). Briefly, cell culture supernatants were centrifuged to remove particulates, and the clarified samples, together with the working solution, were added to the microplates. After washing, the plates were incubated at 37 °C for 2 h, followed by the addition of 100 µL of biotin-conjugated antibody working solution and incubation at 37 °C for 1 h. Subsequently, 100 µL of streptavidin-horseradish peroxidase (HRP) working solution and 100 µL TMB substrate were added to each well sequentially for 30 min and 20 min (in the dark), at 37 °C, respectively. The reaction was terminated by adding 50 µL of the stop solution, and the absorbance was measured at 450 nm using a VICTOR® Nivo™ multimode plate reader (PerkinElmer, Waltham, MA, USA).

Neuron-Glia Co-Culture Assay

To investigate the influence of glial cells on neuronal function, an indirect co-culture system was established using Transwell inserts (#3412, Corning, Corning, NY, USA). Human neuronal SH-SY5Y cells were seeded in the lower chambers of 12-well plates at a density of 5×10^4 cells/well in complete EMEM/F12 medium and pre-cultured for 24 h to allow for cell attachment. Transwell inserts containing pretreated HMC3 glial cells were then carefully transferred into the 12-well plates containing SH-SY5Y cells in the lower chamber. The co-culture was maintained in fresh, serum-free EMEM medium for an additional 48 h. After co-culture, the Transwell inserts (containing HMC3 glial cells) were removed, and the SH-SY5Y cells in the lower chamber were collected for subsequent analyses.

Cell Viability and Apoptosis Assays

Neuronal viability and apoptosis were examined using a commercial Cell Counting Kit-8 (CCK-8) (CA1210, Solarbio, Beijing, China) and an Annexin V-fluorescein isothiocyanate (FITC)/propidium iodide (PI) apoptosis detection kit (CA1020, Solarbio, Beijing, China).

For the cell viability assay, neurons were seeded in 96-well plates at a density of 2×10^3 cells/well and incubated with 10 µL CCK-8 solution for 4 h. The absorbance was measured at 450 nm using a microplate reader. Relative cell viability (%) = $(OD_{experiment} - OD_{blank})/(OD_{control} - OD_{blank}) \times 100\%$.

For the apoptosis assay, 1×10^6 harvested cells were resuspended in 1 mL of 1× binding buffer provided in the kit. After centrifugation to remove the supernatant, the cells were resuspended in the same binding buffer to a final concentration of 1×10^6 cells/mL and incubated with 5 µL each of Annexin V-FITC and PI working solutions for 10 min at room temperature in the dark. Apoptotic cells were analyzed using a CytoFlex flow cytometer (B96622, Beckman Coulter, Indianapolis, IN, USA), and the data were processed using FlowJo 10 software (FlowJo, LLC., Ashland, OR, USA). Apoptosis rate (%) = (percentage of early apoptotic cells) + (percentage of late apoptotic cells).

Co-Immunoprecipitation and In Vitro Deubiquitylation Assays

All procedures for these assays followed previously established methods [20]. Briefly, MG132 solution (20 µM, A2585, ApexBio, Houston, TX, USA) and the antibodies including USP16 (A301-614A, Bethyl Laboratories, Montgomery, TX, USA), IFI16 (#14970, Cell Signaling Technology, Danvers, MA, USA), Flag (30503ES60, Yeasen, Shanghai, China), and HA (ab1424, Abcam, Cambridge, UK) were prepared in advance.

For the co-immunoprecipitation assay, HEK-293T cells were lysed in a lysis buffer containing Tris-HCl (50 mM, AC17151, Acmec Biochemical, China), NaCl (150 mM, S41334, Acmec Biochemical, China), and 1% NP-40 lysis buffer (AC13046, Acmec Biochemical, China) [21], supplemented with phenylmethylsulphonyl fluoride (PMSF, AP0100, Acmec Biochemical, China). The total protein lysates were incubated with an anti-IFI16 antibody (ab169788, 1:10,000, 88 kDa) at 4 °C for 8 h, followed by incubation with protein A/G beads (88802, ThermoFisher Scientific, USA) at 4 °C for 2 h. Whole-cell extracts (WCEs) were prepared as controls. The immunoprecipitated proteins were eluted with 1× SDS buffer (AC13975, Acmec Biochemical, China) and analyzed by western blotting.

For the *in vitro* deubiquitylation assay, HEK-293T cells were transfected with or without USP16-specific shRNA and co-cultured with Flag-IFI16 (#35064, Addgene, Watertown, MA, USA) and HA-Ubiquitin (HA-Ub, #18712, Addgene, USA) for 48 h, followed by MG-132 exposure for 5 h. Cell lysates were prepared using NP-40 lysis buffer containing PMSF. After incubation with the indicated antibodies at 4 °C overnight, WCEs were further incubated with protein A/G beads at 4 °C for 12 h. The bead-bound proteins were eluted with glycine (G12760, Acmec Biochemical, China) prior to the western blot assay.

Western Blotting

Total proteins were extracted using RIPA lysis buffer (AR0010, Acmec Biochemical, China), and their concentrations were determined with a BCA protein assay kit (PC0020, Acmec Biochemical, China). Equal amounts of proteins were separated via SDS-PAGE gel (6% and 8%, AC13342, Acmec Biochemical, China) and transferred to polyvinylidene fluoride membranes (AC17619, Acmec Biochemical, China). The membranes were blocked in 5% skim milk (AD8340, Acmec Biochemical, China) prepared in Tris-buffered saline with Tween 20 (TBS-T; #9997, Cell Signaling Technologies, USA), followed by incubation with primary antibodies (Abcam, UK) against USP16 (ab121650, 1:5000, 94 kDa), IFI16 (ab169788, 1:10,000, 88 kDa), TLR4 (ab218987, 1:10,000, 95 kDa), NLRP3 (ab263899, 1:1000, 118 kDa), and β-actin (ab8226, 1:2000, 42 kDa) overnight at 4 °C. Subsequently, membranes were incubated with HRP-conjugated secondary antibodies (Abcam, UK) against mouse IgG (ab205719, 1:5000) or rabbit IgG (ab205718, 1:5000) at room temperature for 1 h. Protein bands were visualized using the SuperSignal™ West Dura Extended Duration Substrate (34076, ThermoFisher Scientific, USA) and captured with an Odyssey imaging system (version 1.2, LI-COR Biosciences, Lincoln, NE, USA).

Reverse-Transcription Quantitative PCR (RT-qPCR)

After the designated transfection, total RNA was extracted using a total RNA extraction reagent (10606ES60, Yeasen, China) and quantified using a spectrophotometer (ND-LITE, ThermoFisher Scientific, USA). Complementary DNA (cDNA) was synthesized with a commercial reverse transcription kit (K1641, ThermoFisher Scientific, USA). RT-qPCR was performed using an ABI Prism 7500 Fast Real-Time PCR system (Applied Biosystems, Foster City, CA, USA) and SYBR™ Green PCR Master Mix (4309155, Applied Biosystems, USA), under the following thermal cycling conditions: 95 °C for 10 min, followed by 40 cycles of 95 °C for 15 s and 60 °C for 1 min. β-actin served as the internal control, and relative expression levels were calculated using the $2^{-\Delta\Delta Ct}$ method [22]. Primer sequences used are listed in Table 2.

Table 2. Primer sequence used for RT-qPCR.

Gene	Sequence (5′-3′)
IFI16 forward	CTCAGAACCCGAAAACAG
IFI16 reverse	TATTGTGACATTGTCCTGTC
USP16 forward	AAGATCTGAACCTCACTGTC
USP16 reverse	TCCTTTACTCACTCTTTGGT
β-actin forward	CACACCTTCTACAATGAGC
β-actin reverse	ATAGCACAGCCTGGATAG

Notes: RT-qPCR, reverse transcription quantitative polymerase chain reaction; *IFI16*, Interferon gamma-inducible protein 16; *USP16*, ubiquitin-specific peptidase 16.

Statistical Analysis

All experimental data are presented as mean ± standard deviation. Variance homogeneity was verified using Brown-Forsythe test. Comparisons between two groups were performed using an independent samples *t*-test, while multiple-group comparisons were analyzed using one-way analysis of variance (ANOVA) with GraphPad Prism 8.0 (GraphPad, Inc., La Jolla, CA, USA). Tukey test was performed as post-hoc. A p-value < 0.05 was considered statistically significant.

Results

IFI16 Knockdown in Glial Cells Attenuated Aβ1–42-Induced Inflammation and Neuronal Apoptosis

The dataset GSE129296 was first employed to analyze differentially expressed genes (DEGs) in AD, where IFI16 was identified as highly expressed (Fig. 1A). Accordingly, *IFI16*-specific shRNAs (denoted as sh#1–#3 in the figures) were constructed and transfected into HMC3 glial cells, after which the transfection efficiency was evaluated. The data revealed that sh#2 achieved the most effective knockdown (Fig. 1B, $p < 0.05$). Therefore, sh#2 was selected for subsequent experiments and transfected into HMC3 cells prior to Aβ1–42 exposure.

The levels of proinflammatory cytokines (TNF-α and IL-1β) and TLR4/NLRP3 inflammasomes were determined using ELISA (Fig. 1C,D) and western blot analysis (Fig. 1E–G). These inflammation-related markers were significantly elevated following Aβ1–42 exposure (Fig. 1C–G, $p < 0.05$), whereas their expression was notably reduced after IFI16 knockdown (Fig. 1C–G, $p < 0.05$).

To further examine the impact of glial activation on neurons, Aβ1–42-treated glial cells were co-cultured with SH-SY5Y neuronal cells, and neuronal viability and apoptosis were assessed using CCK-8 (Fig. 1H) and flow cytometry (Fig. 1I,J). Exposure to Aβ1–42 markedly reduced neuronal viability and enhanced apoptosis (Fig. 1H–J, $p < 0.05$). Conversely, IFI16 silencing significantly restored neuronal viability and inhibited apoptosis (Fig. 1H–J, $p < 0.05$).

USP16 Acted as the DUBs of IFI16 and Was Highly Expressed in AD

Next, we explored the potential upstream regulator of IFI16 from the perspective of post-translational modification (PTM). Using Ubibrowser, possible deubiquitinating enzymes (DUBs) targeting IFI16 were predicted (Fig. 2A). We then determined the expression level of USP16 in HMC3 glial cells following Aβ1–42 induction and observed a significant increase (Fig. 2B,C, $p < 0.05$). To verify its regulatory role, specific shRNA targeting USP16 were designed and transfected into HMC3 glial cells, among which sh#1 exhibited the most efficient knock-

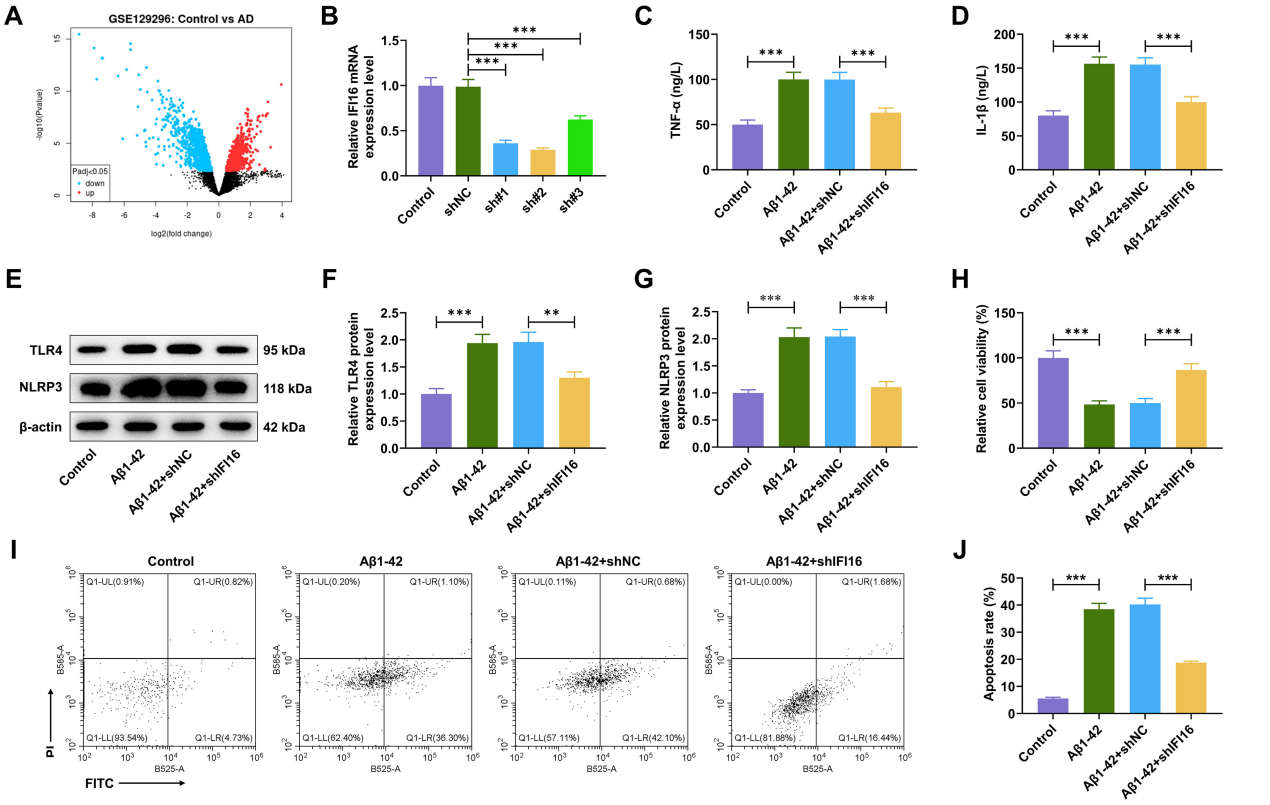

Fig. 1. Knockdown of IFI16, a gene abnormally overexpressed in AD, attenuates Aβ1–42-induced inflammation and neuronal apoptosis in glial cells. (A) The GSE129296 dataset (https://www.ncbi.nlm.nih.gov/geo/query/acc.cgi?acc=GSE129296) retrieved from GEO was used to analyze the differentially expressed genes in AD. (B) Validation of *IFI16*-specific shRNA knockdown efficiency by reverse-transcription quantitative PCR (RT-qPCR). *β-actin* served as the normalization control. (C,D) ELISA was adopted to determine the levels of proinflammatory cytokines TNF-α (C) and IL-1β (D) in HMC3 glial cells following Aβ1–42 induction (5 µM for 24 h) and IFI16 knockdown. (E–G) Based on the analysis of protein grey values (E), the protein expression levels of TLR4 (F) and NLRP3 (G) in HMC3 glial cells following Aβ1–42 induction (5 µM for 24 h) were quantified via western blotting. β-actin served as the normalization control. (H) Following co-culture of HMC3 cells (treated with Aβ1–42, 5 µM for 24 h) and SH-SY5Y neuronal cells, neuronal viability was determined using the CCK-8 assay. (I,J) The apoptosis of SH-SY5Y neuronal cells under the indicated treatments was analyzed by flow cytometry. Data represent the mean ± standard deviation from three independent experiments. Comparison between groups: $^{**}p < 0.01$, $^{***}p < 0.001$. Abbreviation: *IFI16*, interferon gamma inducible protein 16; AD, Alzheimer's disease; shRNA, short hairpin RNA; NC, negative control; Aβ1–42, β-amyloid peptide 1–42; TNF-α, tumor necrosis factor-α; IL-1β, interleukin-1β; ELISA, enzyme-linked immunosorbent assay; TLR4, toll-like receptor 4; NLRP3, NLR family pyrin domain containing 3; CCK-8, cell counting kit-8; FITC, fluorescein isothiocyanate; PI, propidium iodide.

down (Fig. 2D, $p < 0.05$). Moreover, following USP16 silencing, the expression level of IFI16 was markedly reduced (Fig. 2E,F, $p < 0.05$).

Given the role of USP16 as a DUB, we determined the interaction between USP16 and IFI16 and their potential role in IFI16 deubiquitination. Results from co-immunoprecipitation (Fig. 2G) and *in vitro* deubiquitylation assays (Fig. 2H) demonstrated that ectopically expressed USP16 interacted with IFI16, and that the silencing of USP16 enhanced IFI16 ubiquitination (Fig. 2G,H). Furthermore, an IFI16 overexpression plasmid was constructed and transfected into HMC3 cells, with increased IFI16 expression confirming transfection efficiency (Fig. 2I, $p < 0.05$).

USP16 Antagonized IFI16-Mediated Inflammation and Neuronal Damage

Finally, we investigated the interplay between IFI16 and USP16 in Aβ1–42-induced inflammation and apoptosis in glial cells, with or without neuronal cells. The secretion of inflammatory cytokines TNF-α (Fig. 3A) and IL-1β (Fig. 3B) was quantified using ELISA. Both cytokines were significantly upregulated following the overexpression of IFI16 (Fig. 3A,B, $p < 0.05$), while silencing of USP16 reduced their levels and reversed the proinflammatory effects of IFI16 overexpression (Fig. 3A,B, $p < 0.05$). Similarly, the expression of TLR4 and NLRP3 in HMC3 glial cells was quantified following modulation of IFI16 and

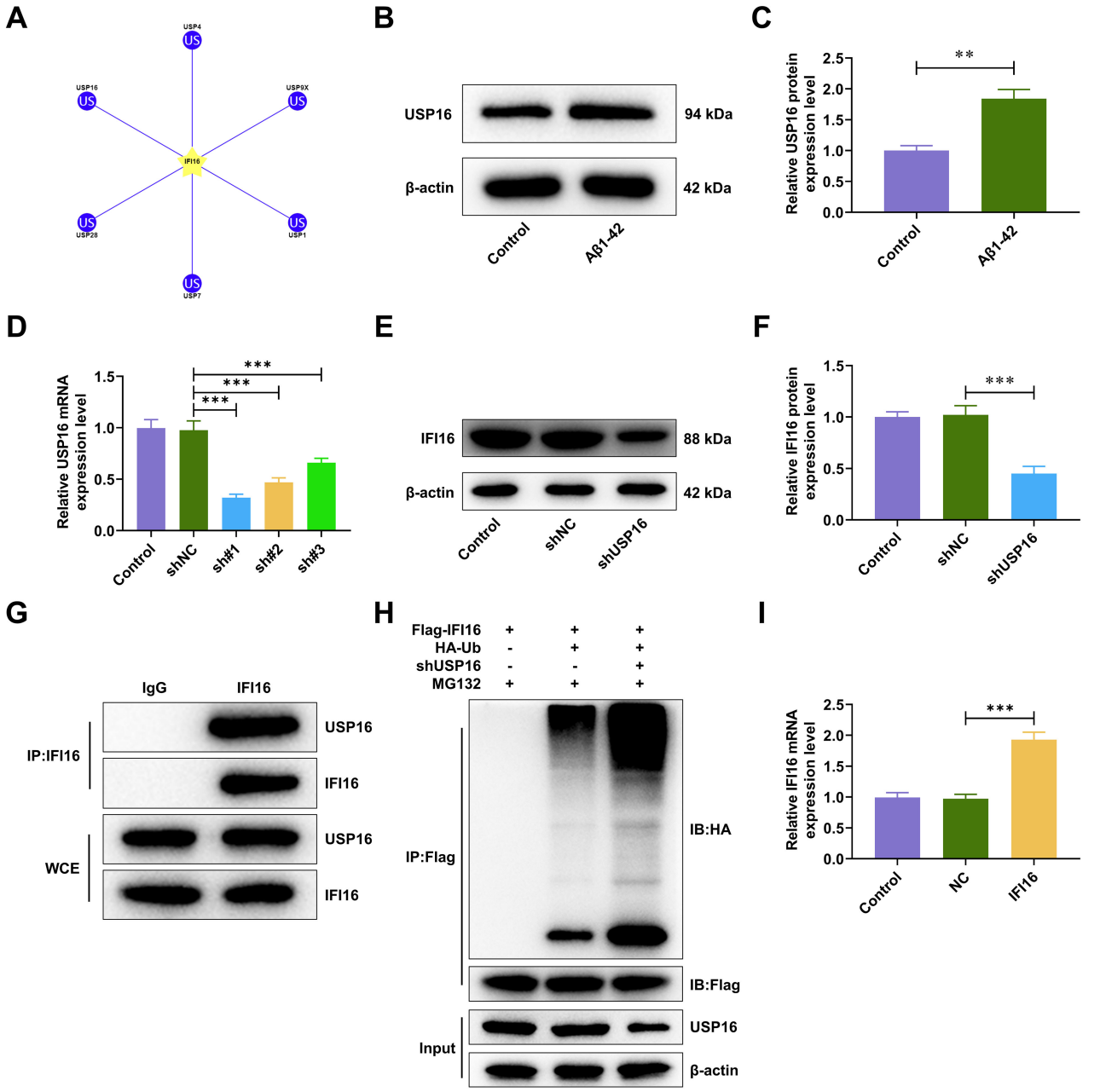

Fig. 2. USP16 functions as the DUBs of IFI16 and is highly expressed in AD. (A) Potential DUBs of IFI16 were predicted using the Ubibrowser database, and interaction factors were ranked clockwise in descending order of confidence scores. (B,C) The protein expression level of USP16 in glial cells following exposure to Aβ1–42 (5 µM for 24 h) was determined by western blot analysis, with β-actin as the normalization control. (D) Validation of USP16-specific shRNA silencing efficiency in HMC3 cells via RT-qPCR. β-actin served as the normalization control. (E,F) Relative protein expression levels of IFI16 in HMC3 cells after USP16 silencing were analyzed by western blot analysis. β-actin served as the normalization control. (G,H) The interaction between USP16 and IFI16, as well as USP16-mediated deubiquitylation of IFI16, was confirmed through co-immunoprecipitation and *in vitro* deubiquitylation assays in HEK-293T cells. (I) Transfection efficiency of the *IFI16* overexpression plasmid in HMC3 cells was determined by RT-qPCR. *β-actin* served as the normalization control. Data represent the mean ± standard deviation from three independent experiments. Comparisons between groups: $^{**}p < 0.01$, $^{***}p < 0.001$. Abbreviation: USP16, ubiquitin-specific peptidase 16; DUBs, deubiquitinating enzymes.

USP16 expression levels. IFI16 overexpression markedly enhanced the protein levels of TLR4 and NLRP3 within the model HMC3 cells (Fig. 3C–E, $p < 0.05$), while USP16 knockdown exerted the opposite effect and mitigated the IFI16-induced overexpression (Fig. 3C–E, $p < 0.05$).

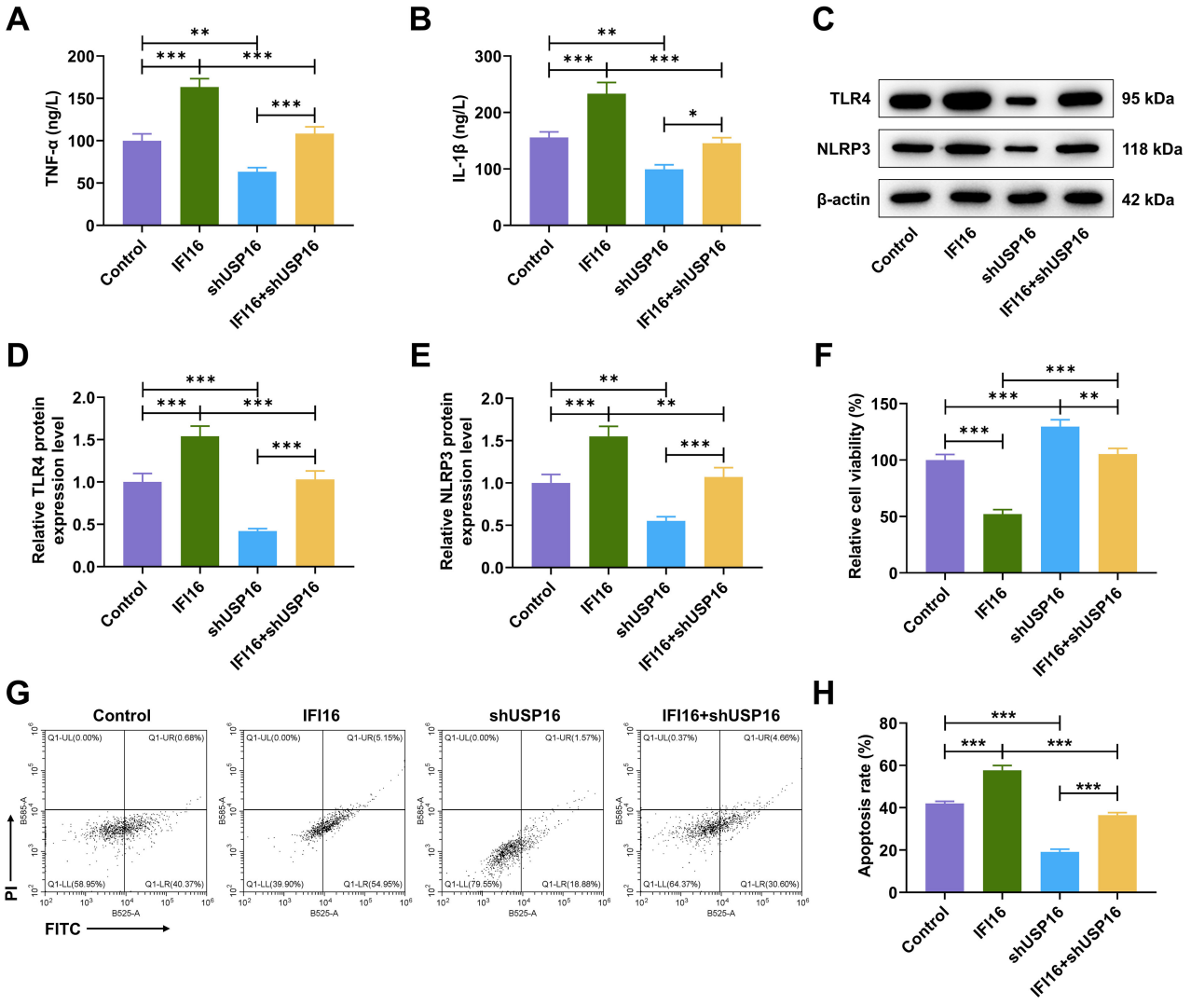

Fig. 3. USP16 knockdown counteracted the effects of IFI16 overexpression on aggravating inflammation and neuronal apoptosis in Aβ1–42-induced AD model cells. (A,B) ELISA was used to determine the levels of proinflammatory cytokines TNF-α (A) and IL-1β (B) in HMC3 glial cells following Aβ1–42 induction (5 μM for 24 h) and IFI16 overexpression and/or USP16 silencing. (C–E) Based on the analysis of protein band grey values (C), the protein expression levels of TLR4 (D) and NLRP3 (E) in HMC3 glial cells following Aβ1–42 induction (5 μM for 24 h) and IFI16 overexpression and/or USP16 silencing were quantified via western blot analysis. β-actin served as the normalization control. (F) Following co-culture of HMC3 cells under the indicated treatments with SH-SY5Y neuronal cells, the viability of SH-SY5Y neuronal cells was determined using the CCK-8 assay. (G,H) The apoptosis of SH-SY5Y neuronal cells under the indicated treatments was determined by flow cytometry. Data represent the mean ± standard deviation from three independent experiments. Comparison between groups: *$p < 0.05$, **$p < 0.01$, ***$p < 0.001$.

Moreover, in the co-culture system, modulation of USP16 and IFI16 expression in glial cells markedly affected neuronal survival. IFI16 overexpression significantly suppressed the viability of SH-SY5Y cells and promoted apoptosis (Fig. 3F–H, $p < 0.05$), whereas USP16 silencing reversed these effects (Fig. 3F–H, $p < 0.05$).

Discussion

Aβ is produced through the cleavage of amyloid precursor protein in the cell membrane by β-secretase and γ-secretase, generating monomeric peptides of varying lengths [23]. Notably, Aβ1–42 present in cerebrospinal fluid (CSF) has been widely recognized as a central biomarker for AD severity, suggesting its potential as a diagnostic marker for the disease [24]. Therefore, Aβ1–42 was employed to establish an *in vitro* AD model in this study, with the aim of further evaluating the effects of the USP16/IFI16 axis on inflammation and apoptosis of these model cells. Based on our findings, we confirmed that silencing IFI16, which was abnormally overexpressed in

AD and deubiquitinated by USP16, attenuated inflammation and apoptosis in AD model cells. These results highlight the regulatory role of the USP16/IFI16 axis in AD pathogenesis and contribute to elucidating the underlying molecular mechanisms involved.

AD is a complex neurodegenerative disorder, with accumulating evidence indicating that both glial and neuronal cells play significant roles in its pathogenesis [25,26]. Moreover, the interaction between neurons and glial cells in AD pathogenesis has been identified as crucial for maintaining synaptic homeostasis [7,27]. Glial cells are vital for sustaining brain homeostasis and play pivotal roles in central nervous system (CNS) injury and diseases, and the inflammation within these cells has been recognized as a crucial factor that disrupts homeostasis and exacerbates AD progression [28,29]. Additionally, neuroinflammation, characterized by glial cell activation, is often indicated by increased expression of inflammatory cytokines, including TNF-α and IL-1β, both of which are early response markers and are expressed concurrently [30].

Among their diverse functions, glial cells regulate synapse formation and respond to neural activity, suggesting that impaired neuron-glia interactions may contribute to the pathogenesis of neurodevelopmental disorders [31,32]. Mechanistically, activation of the TLR4 signaling pathway has been reported to initiate neuroinflammation, with the NLRP3 inflammasome serving as a key mediator [33,34]. Previous studies have shown that IFI16 induces inflammation in hepatitis B virus-associated glomerulonephritis through modulation of the caspase-1/IL-1β pathway and mediates STING signaling as a crucial regulator of anti-HER2 immune responses in HER2-positive breast cancer [35,36]. Moreover, IFI16 has been shown to mediate TNF-α-induced expression of Intercellular Adhesion Molecule 1 (ICAM-1), modulate inflammatory processes, and aggravate LPS-induced TLR4-mediated inflammation, while impacting NLRP3 inflammasome activation to promote inflammation in response to Kaposi's sarcoma-associated herpesvirus infection [37–39].

Nevertheless, the precise role and mechanisms of IFI16 in AD pathogenesis remain insufficiently elucidated. Consistent with our experimental data, IFI16 was significantly upregulated in AD, and its overexpression aggravated inflammation in AD model cells, as evidenced by an increased apoptosis rate and elevated levels of proinflammatory cytokines (TNF-α and IL-1β) and TLR4/NLRP3 signaling components. These findings collectively support the hypothesis that IFI16 contributes to the aggravation of AD through promotion of neuroinflammatory and apoptotic processes.

We next aimed to elucidate the potential underlying mechanism that could further explain the effects of IFI16 on AD. We focused on the specific mechanism of ubiquitination, as its dysregulation has been implicated in various developmental disorders and neurodegenerative diseases [40]. Enzymes, including the DUBs, have been emphasized as key participants in the UPS, where they regulate disease-associated proteins by modulating the degree of ubiquitination [41]. Moreover, DUBs have been shown to counter-regulate the ubiquitination process and influence the stability of neurodegeneration-related pathogenic proteins [17]. Notably, in addition to their potential roles in stabilizing c-Myc [42], histone H2A lysine-119 [43], and calcineurin A [44], USP16 knockdown has been reported to rescue stem cell aging and memory deficits in AD models [18]. We therefore propose that USP16 may aggravate neuroinflammation in AD through deubiquitination of IFI16, thereby enhancing its stability. However, the current study lacks an *in vivo* validation to further validate these findings, which will be the focus of future investigations.

Conclusion

In summary, our findings indicate that the interaction between USP16 and IFI16 through deubiquitylation modulates inflammation and apoptosis in Aβ1–42-induced cellular AD models. This regulatory effect appears to be mediated through the modulation of the TLR4/NLRP3 inflammasome signaling axis.

Availability of Data and Materials

The analyzed data sets generated during the study are available from the corresponding author on reasonable request.

Author Contributions

BC and YD designed the research study. CL performed the research. BC and CL collected and analyzed the data. YD has been involved in drafting the manuscript and all authors have been involved in revising it critically for important intellectual content. All authors gave final approval of the version to be published. All authors have participated sufficiently in the work to take public responsibility for appropriate portions of the content and agreed to be accountable for all aspects of the work in ensuring that questions related to its accuracy or integrity.

Ethics Approval and Consent to Participate

Not applicable.

Acknowledgment

Not applicable.

Funding

This work was supported by Xuanwu Hospital Funding [grant number 303-01-007-0426].

Conflict of Interest

The authors declare no conflict of interest.

References

[1] Srivastava S, Ahmad R, Khare SK. Alzheimer's disease and its treatment by different approaches: A review. European Journal of Medicinal Chemistry. 2021; 216: 113320. https://doi.org/10.1016/j.ejmech.2021.113320.

[2] Swanson CJ, Zhang Y, Dhadda S, Wang J, Kaplow J, Lai RYK, *et al*. A randomized, double-blind, phase 2b proof-of-concept clinical trial in early Alzheimer's disease with lecanemab, an anti-Aβ protofibril antibody. Alzheimer's Research & Therapy. 2021; 13: 80. https://doi.org/10.1186/s13195-021-00813-8.

[3] Breijyeh Z, Karaman R. Comprehensive Review on Alzheimer's Disease: Causes and Treatment. Molecules. 2020; 25: 5789. https://doi.org/10.3390/molecules25245789.

[4] Lei P, Ayton S, Bush AI. The essential elements of Alzheimer's disease. The Journal of Biological Chemistry. 2021; 296: 100105. https://doi.org/10.1074/jbc.REV120.008207.

[5] Calsolaro V, Edison P. Neuroinflammation in Alzheimer's disease: Current evidence and future directions. Alzheimer's & Dementia. 2016; 12: 719–732. https://doi.org/10.1016/j.jalz.2016.02.010.

[6] Heneka MT, Carson MJ, El Khoury J, Landreth GE, Brosseron F, Feinstein DL, *et al*. Neuroinflammation in Alzheimer's disease. The Lancet. Neurology. 2015; 14: 388–405. https://doi.org/10.1016/S1474-4422(15)70016-5.

[7] Nordengen K, Kirsebom BE, Henjum K, Selnes P, Gísladóttir B, Wettergreen M, *et al*. Glial activation and inflammation along the Alzheimer's disease continuum. Journal of Neuroinflammation. 2019; 16: 46. https://doi.org/10.1186/s12974-019-1399-2.

[8] Green R, Mayilsamy K, McGill AR, Martinez TE, Chandran B, Blair LJ, *et al*. SARS-CoV-2 infection increases the gene expression profile for Alzheimer's disease risk. Molecular Therapy Methods & Clinical Development. 2022; 27: 217–229. https://doi.org/10.1016/j.omtm.2022.09.007.

[9] Yi YS, Jian J, Gonzalez-Gugel E, Shi YX, Tian Q, Fu W, *et al*. p204 Is Required for Canonical Lipopolysaccharide-induced TLR4 Signaling in Mice. eBioMedicine. 2018; 29: 78–91. https://doi.org/10.1016/j.ebiom.2018.02.012.

[10] Yang J, Wise L, Fukuchi KI. TLR4 Cross-Talk With NLRP3 Inflammasome and Complement Signaling Pathways in Alzheimer's Disease. Frontiers in Immunology. 2020; 11: 724. https://doi.org/10.3389/fimmu.2020.00724.

[11] Liu Y, Dai Y, Li Q, Chen C, Chen H, Song Y, *et al*. Beta-amyloid activates NLRP3 inflammasome via TLR4 in mouse microglia. Neuroscience Letters. 2020; 736: 135279. https://doi.org/10.1016/j.neulet.2020.135279.

[12] Akimov V, Barrio-Hernandez I, Hansen SVF, Hallenborg P, Pedersen AK, Bekker-Jensen DB, *et al*. UbiSite approach for comprehensive mapping of lysine and N-terminal ubiquitination sites. Nature Structural & Molecular Biology. 2018; 25: 631–640. https://doi.org/10.1038/s41594-018-0084-y.

[13] Sun A, Tian X, Chen Y, Yang W, Lin Q. Emerging roles of the HECT E3 ubiquitin ligases in gastric cancer. Pathology and Oncology Research. 2023; 29: 1610931. https://doi.org/10.3389/pore.2023.1610931.

[14] Weng FL, He L. Disrupted ubiquitin proteasome system underlying tau accumulation in Alzheimer's disease. Neurobiology of Aging. 2021; 99: 79–85. https://doi.org/10.1016/j.neurobiolaging.2020.11.015.

[15] Harris LD, Jasem S, Licchesi JDF. The Ubiquitin System in Alzheimer's Disease. Advances in Experimental Medicine and Biology. 2020; 1233: 195–221. https://doi.org/10.1007/978-3-030-38266-7_8.

[16] Schmidt MF, Gan ZY, Komander D, Dewson G. Ubiquitin signalling in neurodegeneration: mechanisms and therapeutic opportunities. Cell Death and Differentiation. 2021; 28: 570–590. https://doi.org/10.1038/s41418-020-00706-7.

[17] Liu B, Ruan J, Chen M, Li Z, Manjengwa G, Schlüter D, *et al*. Deubiquitinating enzymes (DUBs): decipher underlying basis of neurodegenerative diseases. Molecular Psychiatry. 2022; 27: 259–268. https://doi.org/10.1038/s41380-021-01233-8.

[18] Reinitz F, Chen EY, Nicolis di Robilant B, Chuluun B, Antony J, Jones RC, *et al*. Inhibiting USP16 rescues stem cell aging and memory in an Alzheimer's model. eLife. 2022; 11: e66037. https://doi.org/10.7554/eLife.66037.

[19] Akhter R, Shao Y, Formica S, Khrestian M, Bekris LM. TREM2 alters the phagocytic, apoptotic and inflammatory response to Aβ_{42} in HMC3 cells. Molecular Immunology. 2021; 131: 171–179. https://doi.org/10.1016/j.molimm.2020.12.035.

[20] Zhang Z, Yang H, Wang H. The histone H2A deubiquitinase USP16 interacts with HERC2 and fine-tunes cellular response to DNA damage. The Journal of Biological Chemistry. 2014; 289: 32883–32894. https://doi.org/10.1074/jbc.M114.599605.

[21] Wang YP, Liu IJ, Chen KC, Wu HC. NOTCH1 signaling promotes protein stability of HER3 through the AKT pathway in squamous cell carcinoma of head and neck. Oncogenesis. 2021; 10: 59. https://doi.org/10.1038/s41389-021-00348-5.

[22] Livak KJ, Schmittgen TD. Analysis of relative gene expression data using real-time quantitative PCR and the 2(-Delta Delta C(T)) Method. Methods. 2001; 25: 402–408. https://doi.org/10.1006/meth.2001.1262.

[23] Yang YH, Huang LC, Hsieh SW, Huang LJ. Dynamic Blood Concentrations of Aβ_{1-40} and Aβ_{1-42} in Alzheimer's Disease. Frontiers in Cell and Developmental Biology. 2020; 8: 768. https://doi.org/10.3389/fcell.2020.00768.

[24] Kuhlmann J, Andreasson U, Pannee J, Bjerke M, Portelius E, Leinenbach A, *et al*. CSF Aβ_{1-42} - an excellent but complicated Alzheimer's biomarker - a route to standardisation. Clinica Chimica Acta. 2017; 467: 27–33. https://doi.org/10.1016/j.cca.2016.05.014.

[25] Dzamba D, Harantova L, Butenko O, Anderova M. Glial Cells - The Key Elements of Alzheimer´s Disease. Current Alzheimer Research. 2016; 13: 894–911. https://doi.org/10.2174/1567205013666160129095924.

[26] Goel P, Chakrabarti S, Goel K, Bhutani K, Chopra T, Bali S. Neuronal cell death mechanisms in Alzheimer's disease: An insight. Frontiers in Molecular Neuroscience. 2022; 15: 937133. https://doi.org/10.3389/fnmol.2022.937133.

[27] Bandyopadhyay S. Role of Neuron and Glia in Alzheimer's Disease and Associated Vascular Dysfunction. Frontiers in Aging Neuroscience. 2021; 13: 653334. https://doi.org/10.3389/fnagi.2021.653334.

[28] Donnelly CR, Andriessen AS, Chen G, Wang K, Jiang C, Maixner W, *et al*. Central Nervous System Targets: Glial Cell Mechanisms in Chronic Pain. Neurotherapeutics. 2020; 17: 846–860. https://doi.org/10.1007/s13311-020-00905-7.

[29] Yang QQ, Zhou JW. Neuroinflammation in the central nervous system: Symphony of glial cells. Glia. 2019; 67: 1017–1035. https://doi.org/10.1002/glia.23571.

[30] Teo EJ, Chand KK, Miller SM, Wixey JA, Colditz PB, Bjorkman ST. Early evolution of glial morphology and inflammatory cytokines following hypoxic-ischemic injury in the newborn piglet brain. Scientific Reports. 2023; 13: 282. https://doi.org/10.1038/s41598-022-27034-9.

[31] Herculano-Houzel S. The glia/neuron ratio: how it varies uniformly across brain structures and species and what that means for brain physiology and evolution. Glia. 2014; 62: 1377–1391. https://doi.org/10.1002/glia.22683.

[32] Kim YS, Choi J, Yoon BE. Neuron-Glia Interactions in Neurodevelopmental Disorders. Cells. 2020; 9: 2176. https://doi.org/10.3390/cells9102176.

[33] Alfonso-Loeches S, Ureña-Peralta J, Morillo-Bargues MJ, Gómez-Pinedo U, Guerri C. Ethanol-Induced TLR4/NLRP3 Neuroinflammatory Response in Microglial Cells Promotes Leukocyte Infiltration Across the BBB. Neurochemical Research. 2016; 41: 193–209. https://doi.org/10.1007/s11064-015-1760-5.

[34] Xiao L, Zheng H, Li J, Wang Q, Sun H. Neuroinflammation Mediated by NLRP3 Inflammasome After Intracerebral Hemorrhage and Potential Therapeutic Targets. Molecular Neurobiology. 2020; 57: 5130–5149. https://doi.org/10.1007/s12035-020-02082-2.

[35] Liu L, Xie S, Li C, Guo Y, Liu X, Zhao X, *et al*. IFI16 induces inflammation in hepatitis B virus-associated glomerulonephritis by regulating the Caspase-1/ IL-1 ß pathway. Diagnostic Pathology. 2022; 17: 39. https://doi.org/10.1186/s13000-022-01220-9.

[36] Ong LT, Lee WC, Ma S, Oguz G, Niu Z, Bao Y, *et al*. IFI16-dependent STING signaling is a crucial regulator of anti-HER2 immune response in HER2+ breast cancer. Proceedings of the National Academy of Sciences of the United States of America. 2022; 119: e2201376119. https://doi.org/10.1073/pnas.2201376119.

[37] Sponza S, De Andrea M, Mondini M, Gugliesi F, Gariglio M, Landolfo S. Role of the interferon-inducible IFI16 gene in the induction of ICAM-1 by TNF-alpha. Cellular Immunology. 2009; 257: 55–60. https://doi.org/10.1016/j.cellimm.2009.02.007.

[38] Iannucci A, Caneparo V, Raviola S, Debernardi I, Colangelo D, Miggiano R, *et al*. Toll-like receptor 4-mediated inflammation triggered by extracellular IFI16 is enhanced by lipopolysaccharide binding. PLoS Pathogens. 2020; 16: e1008811. https://doi.org/10.1371/journal.ppat.1008811.

[39] Kerur N, Veettil MV, Sharma-Walia N, Bottero V, Sadagopan S, Otageri P, *et al*. IFI16 acts as a nuclear pathogen sensor to induce the inflammasome in response to Kaposi Sarcoma-associated herpesvirus infection. Cell Host & Microbe. 2011; 9: 363–375. https://doi.org/10.1016/j.chom.2011.04.008.

[40] Rape M. Ubiquitylation at the crossroads of development and disease. Nature Reviews. Molecular Cell Biology. 2018; 19: 59–70. https://doi.org/10.1038/nrm.2017.83.

[41] Do HA, Baek KH. Cellular functions regulated by deubiquitinating enzymes in neurodegenerative diseases. Ageing Research Reviews. 2021; 69: 101367. https://doi.org/10.1016/j.arr.2021.101367.

[42] Ge J, Yu W, Li J, Ma H, Wang P, Zhou Y, *et al*. USP16 regulates castration-resistant prostate cancer cell proliferation by deubiquitinating and stablizing c-Myc. Journal of Experimental & Clinical Cancer Research. 2021; 40: 59. https://doi.org/10.1186/s13046-021-01843-8.

[43] Rong Y, Zhu YZ, Yu JL, Wu YW, Ji SY, Zhou Y, *et al*. USP16-mediated histone H2A lysine-119 deubiquitination during oocyte maturation is a prerequisite for zygotic genome activation. Nucleic Acids Research. 2022; 50: 5599–5616. https://doi.org/10.1093/nar/gkac468.

[44] Zhang Y, Liu RB, Cao Q, Fan KQ, Huang LJ, Yu JS, *et al*. USP16-mediated deubiquitination of calcineurin A controls peripheral T cell maintenance. The Journal of Clinical Investigation. 2019; 129: 2856–2871. https://doi.org/10.1172/JCI123801.